Pergamon

Int. J. Heat Mass Transfer. Vol. 39, No. 9, pp. 1805–1813, 1996

0017–9310/96 $15.00+0.00

0017–9310(95)00278–2

Measurements in buoyancy-opposing laminar flow over a vertical forward-facing step

H. I. ABU-MULAWEH, B. F. ARMALY† and T. S. CHEN

Department of Mechanical and Aerospace Engineering and Engineering Mechanics, University of Missouri-Rolla, Rolla, MO 65401, U.S.A.

(*Received* 23 *January* 1995 *and in final form* 21 *July* 1995)

Abstract—Measurements are reported for buoyancy-opposing laminar mixed convection flow over a vertical, two-dimensional forward-facing step, in which the upstream wall of the step simulated an adiabatic surface, while both the step and the downstream wall from the step were heated to a uniform temperature that was higher than the approaching air temperature. Results presented in this paper are for a step height of 0.8 cm, over a range of free stream velocities $0.39\ \mathrm{m\ s^{-1}} \leqslant u_\infty \leqslant 0.71\ \mathrm{m\ s^{-1}}$ and a range of temperature differences $0°\mathrm{C} \leqslant \Delta T \leqslant 35°\mathrm{C}$ between the heated surface and the free stream. Laser–Doppler velocimeter and cold-wire anemometer were used to measure, respectively, the air velocities and the temperature distributions simultaneously. Flow visualizations were also used to observe the nature of the flow and to measure the length of the recirculation region downstream of the forward-facing step. The results reveal that the buoyancy-opposing force due to the downstream wall heating affects significantly the velocity and temperature distributions, the local Nusselt number, and the location and the size of the recirculation region downstream of the step.

INTRODUCTION

Flow separation arising from a sudden change in flow geometry, such as forward-facing step, plays an important role in the design of many heat transfer devices, such as cooling systems for electronic equipment, high performance heat exchangers, combustion chambers, chemical processes and energy systems equipment, and cooling passages of turbine blades. The forward-facing step flow geometry has been examined numerically in the past; see, for example, Fletcher and Srinivas [1] and Baron *et al.* [2]. Recently, laminar mixed convection flow over horizontal and vertical forward-facing steps has been studied experimentally by Abu-Mulaweh *et al.* [3, 4]. All of these mixed convection studies on the forward-facing step have considered only the case of buoyancy-assisting flow condition. The case of buoyancy-opposing flow condition seems not to have been investigated in the past and this has motivated the present study.

The present study extends the work of Abu-Mulaweh *et al.* [3, 4] and deals with buoyancy-opposing, two-dimensional (2D), laminar air flow over a vertical forward-facing step under the mixed convection condition. The step and the wall downstream of the step are heated and maintained at a uniform temperature while the upstream wall is kept adiabatic. Results of interest, such as velocity and temperature distributions, recirculation region lengths, and local Nusselt numbers are reported to illustrate the effects of the buoyancy-opposing force (i.e. wall-free stream temperature difference) and the free stream velocity on these parameters.

EXPERIMENTAL APPARATUS AND PROCEDURE

The experimental study was performed in an existing low-turbulence, open-circuit air tunnel. Details of the air tunnel have been described by Ramachandran *et al.* [5]. In this experiment, the forward-facing step geometry was identical to that used by Abu-Mulaweh *et al.* [3, 4], except that the orientation of the air tunnel was changed by 180° to create buoyancy-opposing flow conditions as shown in Fig. 1. The test geometry consisted of a heated forward-facing step geometry, with an adiabatic upstream section (20.0 cm long × 30.48 cm wide), a heated (constant temperature) forward-facing step and downstream section (79 cm long × 30.48 cm wide) behind the step, which spanned the total width of the air tunnel. The test section of the air tunnel is instrumented with laser–Doppler velocimeter (LDV) and cold wire anemometer to measure the velocity and temperature distributions simultaneously, as described by Baek *et al.* [6]. The heated wall of the test geometry was constructed of four layers which were held together by screws and instrumented to provide an isothermal heated surface. The upper layer was an aluminum plate instrumented with 18 copper–constantan thermocouples that were distributed in both the axial and the transverse directions. Each thermocouple was inserted into a hole on the backside of the plate and its measuring junction was flush with the test surface. The second layer consisted of five separately con-

† Author to whom correspondence should be addressed.

NOMENCLATURE

g	gravitational acceleration
Gr_s	Grashof number, $g\beta(T_w - T_\infty)s^3/\nu^2$
h	heat transfer coefficient, $-k(\partial T/\partial y)_{y=0}/(T_w - T_\infty)$
H	height of computational domain at inlet section
k	thermal conductivity
Nu_s	local Nusselt number, hs/k
p	pressure
P	dimensionless pressure, $(p+\rho gx)/(\rho_o u_o^2)$
Pr	Prandtl number, ν/α
Re_s	Reynolds number, $u_\infty s/\nu$
s	step height
T	fluid temperature
T_∞	free stream temperature
T_w	heated wall temperature
u	streamwise velocity component
u_∞	free stream velocity
U	dimensionless streamwise velocity component, u/u_∞
v	transverse velocity component
V	dimensionless transverse velocity component, v/u_∞
x, y	streamwise and transverse coordinates measured from the upper corner of the step
X, Y	dimensionless and streamwise transverse coordinates, x/s, y/s
x_e	length of the computational domain downstream from the step
x_i	length of the computational domain upstream from the step
x_r	length of the laminar non-circulating flow region downstream from the step
x_t	distance from the step where turbulent flow starts to develop
X_e, X_i, X_r, X_t	x_e/s, x_i/s, x_r/s, x_t/s.

Greek symbols

α	thermal diffusivity
β	volumetric thermal expansion coefficient
δ_s	boundary layer thickness at the step, $5x_i/Re_{xi}^{1/2}$
ΔT	temperature difference, $(T_w - T_\infty)$
θ	dimensionless temperature, $(T - T_\infty)/(T_w - T_\infty)$
ν	kinematic viscosity
ρ	density.

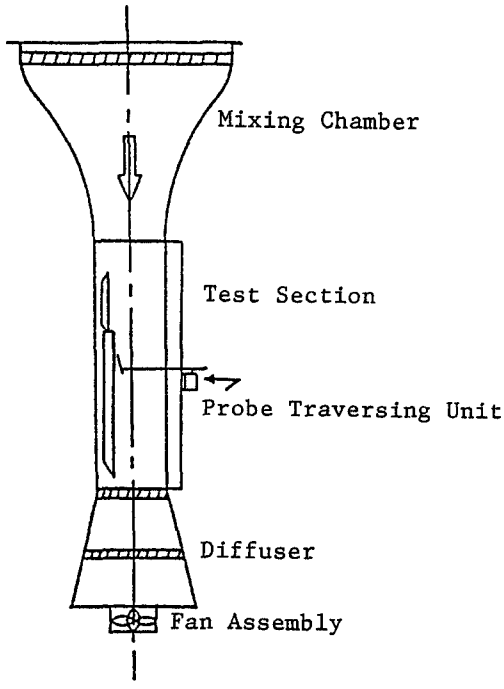

Fig. 1. Schematic diagram of the air tunnel.

trolled heater pads, and an insulation layer formed the third layer. The bottom layer was an aluminum plate which served as backing and support for the structure of the plate. The front edge of this heated plate was squared to form the heated forward-facing step. The upstream section of the forward-facing step geometry was constructed from Plexiglass which was simulated numerically as an adiabatic surface. Minimum contact was achieved between the upstream plate and the step by chamfering the Plexiglass surface, thus minimizing the heat transfer between the two surfaces. The freestream air velocity in the tunnel could be varied between 0.25 and 3.0 m s^{-1} and the heated downstream plate could be maintained at a uniform and constant temperature between 25 and 75°C by controlling the power input to the individual heaters. The repeatability of the air velocity measurements was within 3%, and that of the temperature measurements was within 0.05°C.

Flow visualizations were performed, by using a 15 W collimated white light beam, 2.5 cm in diameter, to examine the nature of the flow and to measure the length of the recirculating flow region. The flow was seeded with Glycerin particles, 2–5 μm in diameter, which served as scattering centers for flow visualization and for LDV measurements.

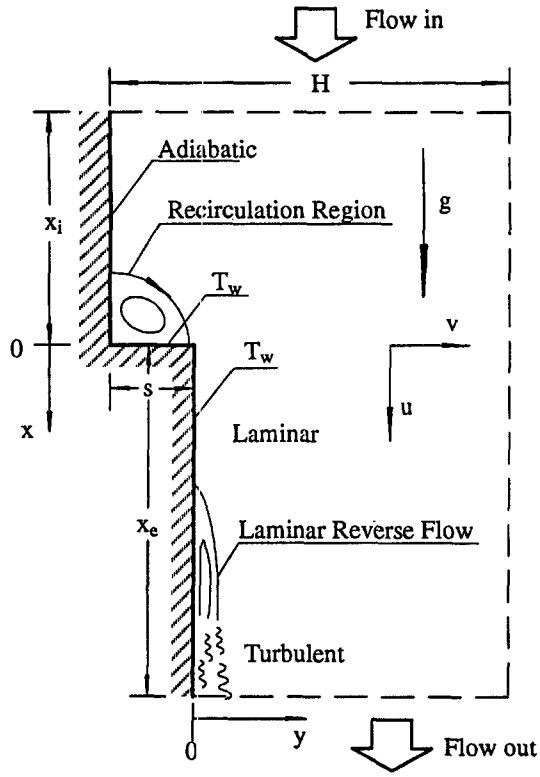

Fig. 2. Schematic diagram of the calculation domain.

NUMERICAL ANALYSIS

The experimental geometry and boundary conditions were also modeled for numerical simulation, as shown in Fig. 2. The upstream wall was considered as adiabatic, while the wall downstream of the step and the step itself were considered as being heated to a uniform temperature T_w. The gravitational acceleration g is acting vertically downward. The thermal properties were considered to be constant but evaluated at the film temperature $T_f = (T_w + T_\infty)/2$.

By utilizing the Boussinesq approximation ($\beta\Delta T < 0.1$ in this experiment), the governing conservation equations for the physical problem under consideration can be written in dimensionless form as follows:

$$\partial U/\partial X + \partial V/\partial Y = 0 \tag{1}$$

$$U\partial U/\partial X + V\partial U/\partial Y = -\partial P/\partial X + (1/Re_s)(\partial^2 U/\partial X^2 + \partial^2 U/\partial Y^2) - (Gr_s/Re_s^2)\theta \tag{2}$$

$$U\partial V/\partial X + V\partial V/\partial Y = -\partial P/\partial Y + (1/Re_s)(\partial^2 V/\partial X^2 + \partial^2 V/\partial Y^2) \tag{3}$$

$$U\partial\theta/\partial X + V\partial\theta/\partial Y = (1/PrRe_s)(\partial^2\theta/\partial X^2 + \partial^2\theta/\partial Y^2). \tag{4}$$

The boundary conditions are given by:

At inlet:

$$-1 < Y < H/s - 1 \quad X = -X_i: \quad U = 1 \quad V = \theta = 0 \tag{5}$$

At exit:

$$0 < Y < H/s - 1 X = X_e: \quad U, V \text{ and } \theta \text{ measured values} \tag{6}$$

Upstream wall:

$$Y = -1 \quad -X_i < X < 0: \quad U = V = 0 \quad \partial\theta/\partial Y = 0 \tag{7}$$

Step wall:

$$-1 < Y < 0 \quad X = 0: \quad U = V = 0 \quad \theta = 1 \tag{8}$$

Downstream wall:

$$Y = 0 \quad 0 < X < X_e: \quad U = V = 0 \quad \theta = 1 \tag{9}$$

Flat wall:

$$Y = H/s - 1 \quad -X_i < X < X_e: \quad U = V = \theta = 0. \tag{10}$$

For the calculation domain, the upstream length x_i, the downstream length x_e, the height of the upstream flow domain H, and the step height s were 20.0 cm, 15.0 cm, 15.0 cm and 0.8 cm, respectively. The lengths x_i, H and s are identical with the same parameters of the experimental geometry, but x_e is smaller than the experimentally heated downstream plate which was equal to 79 cm. The solution procedure, convergence criterion, grid distributions and numerical uncertainties are presented and discussed by Baek *et al.* [6].

RESULTS AND DISCUSSION

The uniformity and the 2D nature of the flow were verified through flow visualizations and through measurements of velocity and temperature across the width of the air tunnel, at various heights above the test surface. These measurements displayed a wide region, about 80%, around the center of the tunnel's width where the flow could be approximated (to within 5%) as being two-dimensional. All reported streamwise velocity and temperature distributions in the transverse, y, direction were taken along the midplane ($z = 0$) of the plate's width, and only after the system had reached steady-state conditions.

Flow visualizations were conducted to determine the general nature of the flow and to observe the effects of the opposing buoyancy force on it. For the case of an approaching laminar forced convection flow (i.e. $\Delta T = 0°C$) the following observations were made:

(1) When $\delta_s/s > 1.15$, a laminar recirculating flow region develops upstream of the step and a laminar

flow with no recirculating flow regions was observed downstream of the step.

(2) When $0.7 < \delta_s/s < 1.15$, a laminar recirculating flow region develops upstream of the step and a small shallow laminar recirculating flow region develops downstream of the step.

(3) When $\delta_s/s < 0.7$, a laminar recirculating flow region develops upstream of the step and the transition from laminar to turbulent flow starts to develop at the lower end of the recirculating flow region that develops downstream from the step.

The present study examines the effects of opposing buoyancy force (i.e. $\Delta T > 0$°C) for the case where $\delta_s/s > 1.15$ with laminar approaching flow. This regime was selected because it exhibits a laminar flow region downstream of the step which can be influenced significantly by increasing the buoyancy-opposing force. It offers the opportunity to observe and study the transition of the flow from laminar to turbulent which is caused by the buoyancy-opposing force. Qualitatively, the following flow characteristics were observed from the flow visualization studies:

(1) When $u_\infty > 0$ and the temperature of the downstream plate is the same as the free stream temperature (i.e. $\Delta T = 0$°C), there is no opposing buoyancy force and the flow is equivalent to a forward-facing step forced flow as described by Abu-Mulaweh *et al.* [4]. The flow is laminar and does not have any recirculating flow regions downstream of the step.

(2) When the freestream velocity, u_∞, is zero and the downstream plate is heated ($\Delta T > 0$°C), the flow is equivalent to natural convection boundary layer flow adjacent to a vertical flat plate. Here again the flow is laminar and does not have any recirculating flow regions downstream from the step. The direction of the induced flow for this condition is opposite to the direction of the forced convection flow imposed in the above case 1. The conditions in 1 and 2 represent the two extremes, forced convection and natural convection flows in this geometry.

(3) When both $u_\infty > 0$ and $\Delta T > 0$°C, the mixed convection buoyancy opposing flow regime prevails. In such a situation a laminar approaching forced flow is imposed in the downward direction and a buoyancy-opposing induced flow develops in the opposite direction, and these two flow streams interact with each other. The interaction of these two flows causes the development of three distinct flow regions adjacent to the heated plate downstream of the step: a laminar flow region without any recirculating flow, a laminar recirculating flow region, and a turbulent flow region, as shown in Fig. 2. As the bouyancy opposing force increases as a result of increase in the wall temperature of the downstream plate, the laminar recirculating flow region moves closer to the step and its length decreases. In addition, the turbulent region that develops at the lower end of the laminar recirculating flow region moves closer to the step as the opposing buoyancy force increases. This behavior is similar to the one reported by Abu-Mulaweh *et al.* [7] for buoyancy opposing flow adjacent to a flat plate, and the observed results from this study are quantified in Fig. 3. In Fig. 3 the solid line represents the length, X_r, of the laminar non-circulating flow region downstream of the step (i.e. the location downstream of the step at which the laminar recirculation region starts), while the dashed line represents the end of the laminar recirculation region (i.e. the location downstream from the step at which the turbulent flow region starts, X_t). It can be seen from the figure that the length of laminar non-circulating flow region, X_r, and the length of the laminar recirculating flow region (X_t–X_r) decrease rapidly as the buoyancy level Gr_s/Re_s^2 increases because of a decrease in the free streamwise velocity and/or an increase in the downstream wall heating. The uncertainty in X_r and X_t is ± 0.25 and in Gr_s/Re_s^2 is $\pm 4 \times 10^{-5}$.

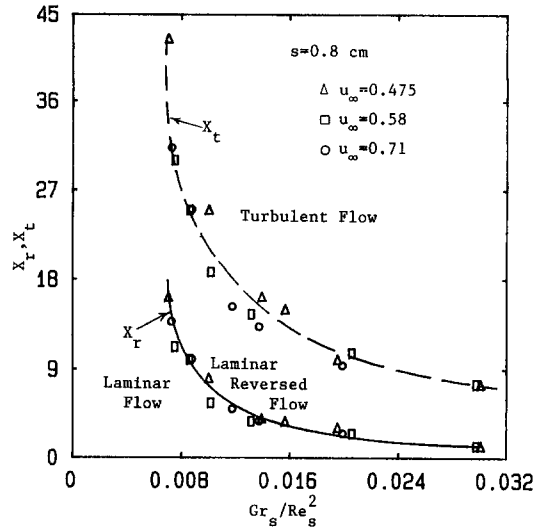

Fig. 3. Effect of buoyancy force on the recirculation region downstream of the step (uncertainty in X_r and X_t is ± 0.25 and in Gr_s/Re_s^2 is $\pm 4 \times 10^{-5}$).

The measured and the predicted velocity and temperature distributions at four different locations downstream from the step are presented in Fig. 4. In the figure, the different symbols and the solid lines, respectively, represent the measured and the predicted results. As can be seen from the figure, the velocity gradients at the wall are positive for all velocity distributions, indicating that these locations are in the laminar non-circulating flow region downstream from the step. As expected, the velocity and the temperature gradients at the wall decrease as the downstream location from the step increases. Good agreement exists between the measured and the predicted velocity and temperature results (within 5%). The uncertainty in u/u_∞ is ± 0.014, in θ is ± 0.025 and in y/s is ± 0.022.

The effects of buoyancy-opposing force, from downstream wall heating, on the streamwise velocity distributions at three different downstream locations are shown in Fig. 5. It was found that whenever the

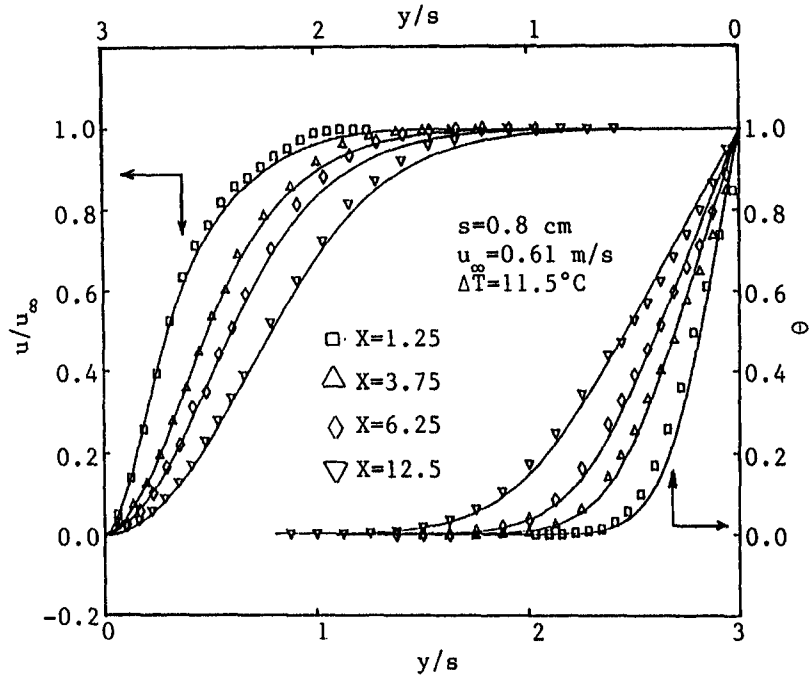

Fig. 4. Dimensionless axial velocity and temperature distributions downstream of the step (uncertainty in u/u_∞ is ± 0.014, in θ is ± 0.025 and in y/s is ± 0.022).

exit boundary of the calculation domain, as expressed in equation (6) at $x_e = 15.0$ cm, is larger than the laminar non-circulating flow region (i.e. $x_e > x_r$) the predicted numerical results deviate significantly from measured values and for that reason they are not presented for comparison. This deviation probably arises from the fact that the measured values at the exit plane for these conditions do not completely and uniquely specify the state of the flow at the exit plane (vertical velocity component was not measured) and are strongly affected by the downstream conditions, and for that reason the numerical model fails to predict the measured results in the calculation domain. The same results were observed by Abu-Mulaweh *et al.* [8] for the case of backward-facing steps under buoyancy-opposing flow conditions. Figure 5 clearly shows that numerical predictions agree favorably well with the measured results for the cases of $\Delta T = 0$ and 11.5°C. For these cases the exit boundary condition of the calculation domain ($x_e = 15$ cm) is in the laminar non-circulating flow region downstream of the step. As can be seen from the figure, the effect of downstream wall heating increases as the streamwise distance from the step increases. The velocity gradient at the wall decreases as the wall heating increases (i.e. as buoyancy-opposing force increases), and some of the velocity distributions exhibit negative velocities close to the wall, indicating that these locations for the given heating conditions are inside the laminar recirculating flow region. In the recirculation flow region, the velocity gradient at the wall increases in the negative sense as the downstream wall heating increases, which is accompanied by an increase in the thickness of the recirculation region.

Figure 6 illustrates the effect of the free stream velocity on the velocity distributions at four different downstream locations. It should be noted that for the given conditions in the figure the exit plane of the calculation domain (i.e. $x_e = 15$ cm) is inside the laminar recirculating flow region and for that reason numerical predictions are not presented for comparison in this figure. The figure shows that as the free stream velocity decreases (i.e. increasing buoyancy opposing force) the thickness of the recirculating flow region increases, and that region moves closer towards the step. For example, at $X = 6.25$ there is no negative velocity for $u_\infty = 0.61$ m s^{-1}, which indicates that the laminar recirculating flow region is downstream of this location. On the other hand, for $u_\infty = 0.51$ m s^{-1} and 0.39 m s^{-1}, there exists negative velocity at $X = 6.25$, indicating that the laminar recirculating flow region occurs upstream of this location for these two free stream velocities, with the smaller u_∞ giving rise to a smaller X_r (see Fig. 3). The velocity distribution at $X = 12.5$ for the free stream velocity of 0.39 m s^{-1} is not shown in the figure because the flow becomes turbulent at this location for the given conditions.

The effects of buoyancy force, from downstream wall heating, on the temperature distributions at four different locations are shown in Fig. 7. In the laminar non-circulating flow region downstream from the step

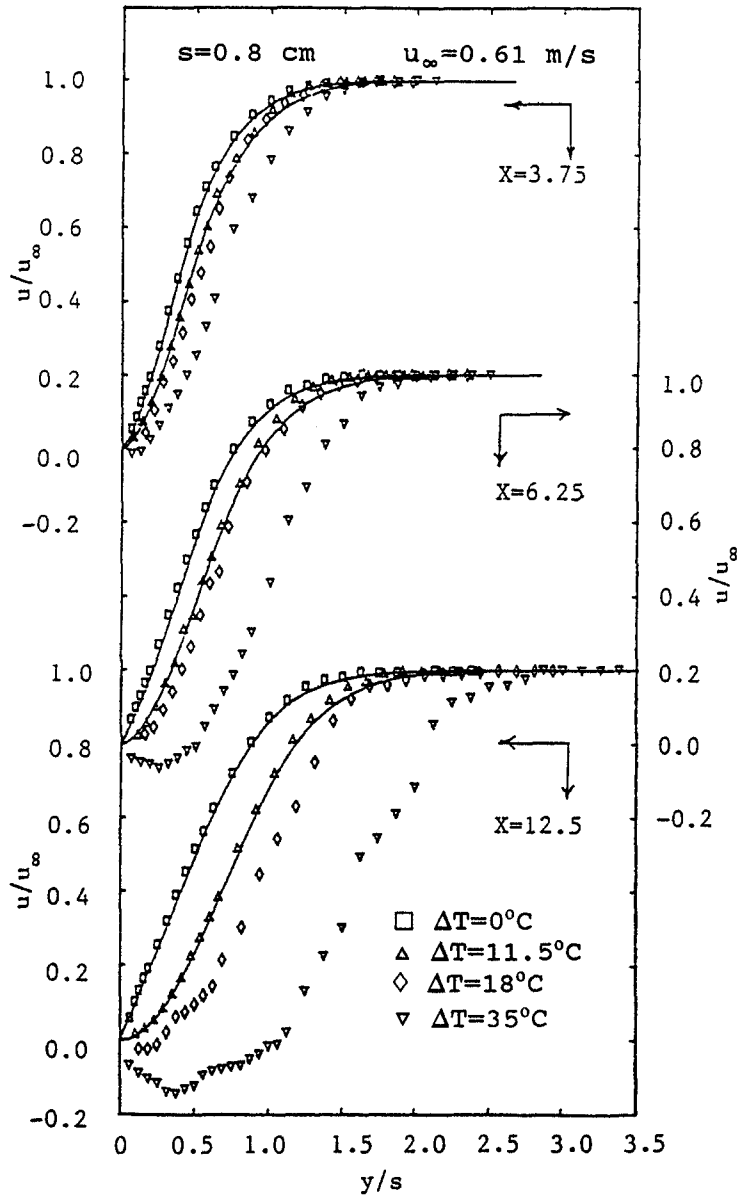

Fig. 5. Effects of downstream wall heating on the velocity distributions (uncertainty in u/u_∞ is ± 0.014 and in y/s is ± 0.022).

($X = 1.25$ and 3.75), the temperature gradient at the heated wall decreases (i.e. the heat transfer rate decreases) as the temperature difference increases. This is the opposite to what was observed for the buoyancy assisting case. On the other hand, inside the recirculation region ($X = 6.25$ and 12.5) the reverse is true (i.e. the temperature gradient at the heated wall increases with increasing temperature difference). This is because the recirculating flow region is being fed by a lower temperature fluid that is moved by the buoyancy induced flow, thus causing a larger temperature gradient.

Figure 8 illustrates the effects of buoyancy force, from downstream wall heating, on the axial variation of the local Nusselt number. A good agreement exists (within 8%) between the predictions (solid line) and the measured results for the case of $\Delta T = 11.5$°C. For the conditions that are presented in the figure, the local Nusselt number decreases as the buoyancy force increases in the region of $X < 5$ (i.e. the laminar non-circulating flow region), while this trend is seen to reverse inside the laminar recirculating flow region ($X > 5$). The uncertainty in the experimentally determined Nu_s is ± 0.05 and in X is ± 0.05.

CONCLUSIONS

Measurements of velocity and temperature distributions for buoyancy-opposing, laminar mixed

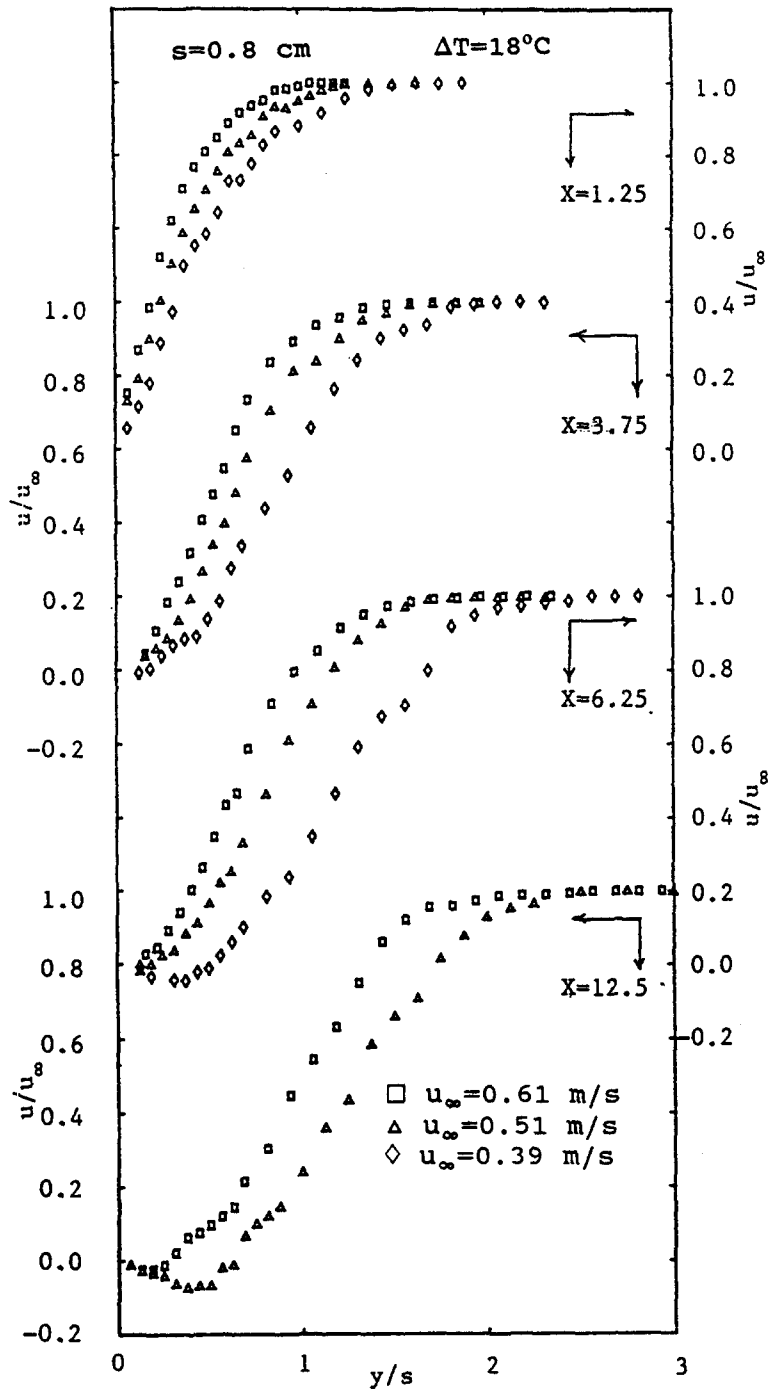

Fig. 6. Effect of free stream velocity on the velocity distributions (uncertainty in u/u_∞ is ± 0.014 and in y/s is ± 0.022).

convection flow over a vertical foward-facing step are reported. The results reveal that the opposing buoyancy force affects significantly the location and length of the recirculating flow region downstream of the step as well as the local Nusselt number. It has been found that the recirculating flow region downstream of the step moves towards the step and its length decreases as the downstream wall heating increases. In the laminar non-circulating flow region downstream of the step, the local Nusselt number decreases with increasing opposing buoyancy force and the reverse trend may occur inside of the recirculating

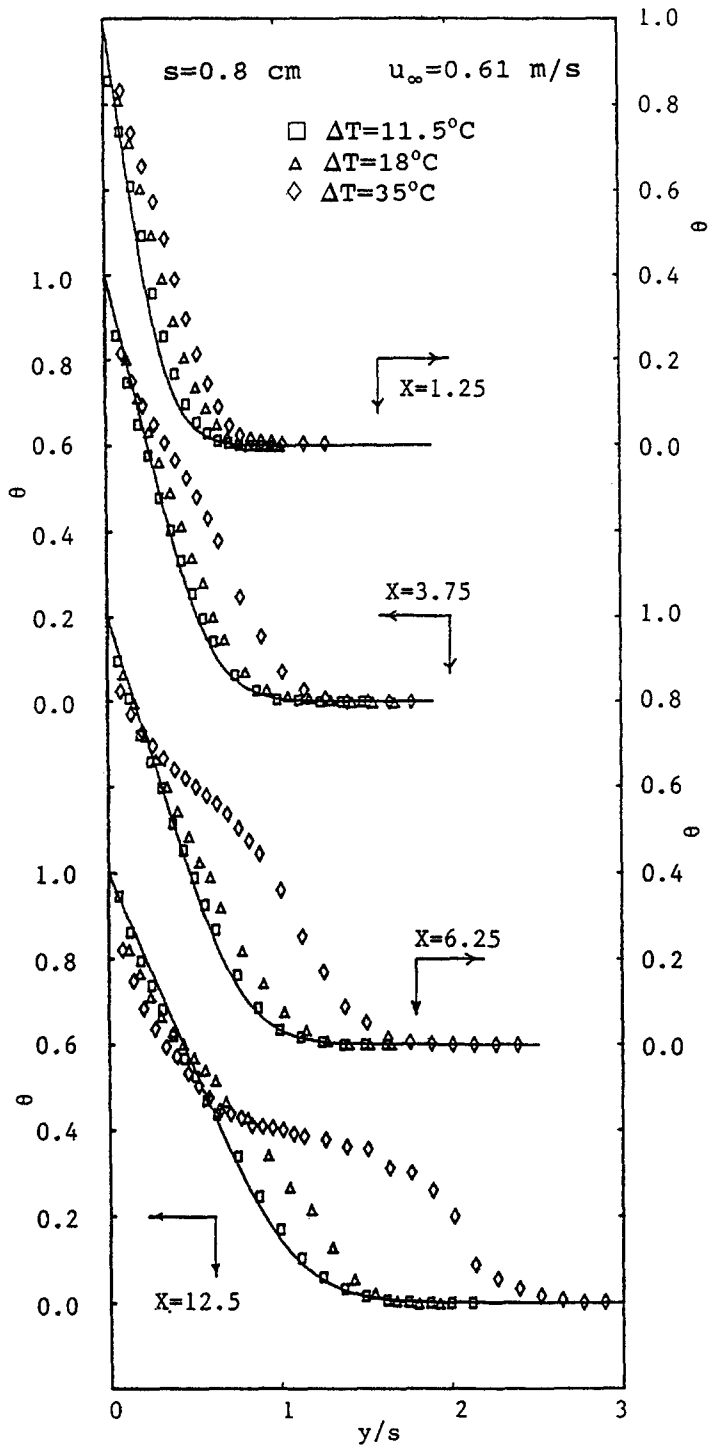

Fig. 7. Effects of downstream wall heating on the temperature distributions (uncertainty in θ is ± 0.025 and in y/s is ± 0.022).

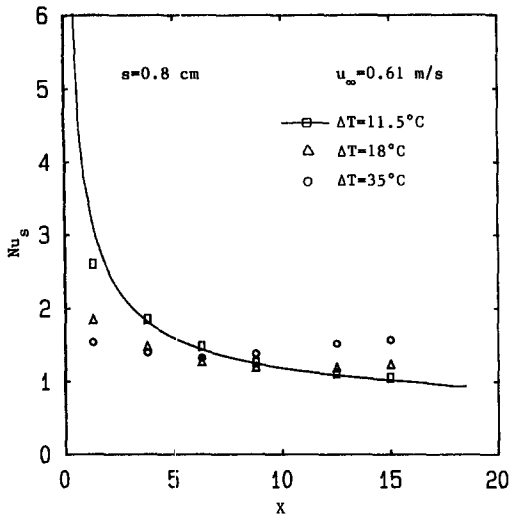

Fig. 8. Effects of downstream wall heating on the axial variation of the Nusselt number (uncertainty in Nu_s is ± 0.05 and in X is ± 0.05).

flow region. This is opposite to the trend observed for the buoyancy assisting case.

Acknowledgements—The present study was supported in part by a grant from the National Science Foundation (NSF CTS—9304485). Mr. Bin Hong assisted in the numerical computations.

REFERENCES

1. C. A. J. Fletcher and K. Srinivas, Stream function vorticity revisited, *Comput. Meth. Appl. Mech. Engng* **41**(3), 297–322 (1983).
2. A. Baron, F. K. Tsou and W. Aung, Flow field and heat transfer associated with laminar flow over a forward-facing step, *Proceedings of the 8th International Heat Transfer Conference*, Vol. 3, pp. 1077–1082. Hemisphere, Washington, DC (1986)
3. H. I. Abu-Mulaweh, B. F. Armaly and T. S. Chen, Measurements of laminar mixed convection flow over a horizontal forward-facing step, *J. Thermophys. Heat Transfer* **7**(4), 569–573 (1993).
4. H. I. Abu-Mulaweh, B. F. Armaly, T. S. Chen and B. Hong, Mixed convection adjacent to a vertical forward-facing step, *Proceedings of the 10th International Heat Transfer Conference*, Brighton, U.K. (Edited by G. F. Hewitt), Vol. 5, pp. 423–428 (1994).
5. N. Ramachandran, B. F. Armaly and T. S. Chen, Measurements and predictions of laminar mixed convection flow adjacent to a vertical surface. *J. Heat Transfer* **107**(3), 636–641 (1985).
6. B. J. Baek, B. F. Armaly and T. S. Chen, Measurements in buoyancy-assisting separated flow behind a vertical backward-facing step, *J. Heat Transfer* **115**(2), 403–408 (1993).
7. H. I. Abu-Mulaweh, B. F. Armaly and T. S. Chen, Instabilities of mixed convection flows adjacent to inclined plates, *J. Heat Transfer* **109**(4), 1031–1033 (1987).
8. H. I. Abu-Mulaweh, B. F. Armaly and T. S. Chen, Measurements in buoyancy-opposing laminar flow over a vertical backward-facing step, *J. Heat Transfer* **116**(1), 247–250 (1994).